Light absorption spectra in oligothiophene molecules

Fabrizio Gala, and Giuseppe Zollo

Citation: AIP Conference Proceedings **1873**, 020001 (2017); doi: 10.1063/1.4997130
View online: https://doi.org/10.1063/1.4997130
View Table of Contents: http://aip.scitation.org/toc/apc/1873/1
Published by the American Institute of Physics

Light Absorption Spectra in Oligothiophene Molecules

Fabrizio Gala and Giuseppe Zollo[a)]

Dipartimento di Scienze di Base e Applicate per l'Ingegneria, Universitá di Roma "La Sapienza", Via A. Scarpa 14–16, 00161 Rome Italy

[a)]Corresponding author: giuseppe.zollo@uniroma1.it

Abstract. First principles calculations based on density functional theory, density functional perturbation theory and many body perturbation theory are employed to explain the optical absorption peak of a newly synthesized oligo-tiophene molecule that has been considered for bulk-heterojunction solar cells. The GW approach is used to obtain quasiparticle energies as a pre-requisite to solve the Bethe-Salpeter equation for the excitonic Hamiltonian, while density functional perturbation theory, in conjunction with the Huang-Rhys method, have been employed to calculate the vibration assisted ionization spectrum.

INTRODUCTION

Organic cells have many appealing properties such as: low fabrication cost, solution processability, transparency and flexibility that make them appealing for solar energy conversion Moreover, power conversion efficiencies (PCEs) of polymer based solar cells (PSCs) with bulk-heterojunction (BHJ) architecture have been greatly improved in the recent years [1].

In BHJ materials [2] light absorption at the donor generates strongly bound Frenkel-type excitons[3, 4] that, at the donor-acceptor interface, have to be separated to generate the electrical current between the electrodes. Fullerene derivates are commonly considered as good acceptors BHJs while good donor materials are still under intense research to improve the organic solar cells performances.

In particular, π-conjugated small molecules, made of a push-pull structure with an electron-donating central unit (D) and peripheral electron-accepting groups (A) as end groups, have been considered as donors in BHJ solar cells, with an increased PCE up to 9∼10% [5–8] in the last years. However, solution-processed small molecule organic solar cells have not reached these performances so far. On the other hand, their properties of manageable synthesis and stability, high purity, batch to batch control, and easier energy level design are quite attractive and that's why research is pushing on them, especially concerning the quantitative understanding of the exciton formation [5, 9–11] that is still poor.

Indeed, accurate description of electron-hole (eh) interactions could be addressed in the context of quantum-chemical approaches but with prohibitive computational effort. Alternatively, Many-body perturbation theory (MBPT) techniques, namely the GW approximation[12] and the Bethe-Salpeter equation (BSE), ensure good accuracy with reasonable computational cost and have been already employed in organic crystals and small molecules [13–18].

It should be stressed, however, that some relatively important phenomena, such as dynamical effects in exciton screening or electron-phonon coupling, are not included in the GW-BSE scheme. Among them, the absorption peak shape that is related to the so called Frank-Condon (FC) effect due to vibrational modes of the molecule in its ground and excited states.

In this work we study the full absorption spectrum of a modified version of the BT2N molecule, the diethyl 3,3'-(3,3"'-dioctyl-[2,2':5',2":5",2"'-quaterthiophene]-5,5"'-diyl)(2E,2'E)-bis(2-cyanoacrylate), with chemical formula $C_{44}H_{52}N_2O_4S_4$, a newly assembled oligomer-like molecule for organic solar cells. BT2N has been already considered showing that the absorption spectrum can be explained if a π-stacking between the molecules is taken into account [18]. However in this previous work, only the peak position was taken into account and no attempt to predict the peak broadening and shape was performed. The molecule here considered (BT2Na in the following) has the following chemical formula $C_{28}H_{20}N_2O_4S_4$ and has been obtained from BT2N by removing the aliphatic chains. The

NANOINNOVATION 2016
AIP Conf. Proc. 1873, 020001-1–020001-10; doi: 10.1063/1.4997130
Published by AIP Publishing. 978-0-7354-1553-9/$30.00

absorption spectrum is calculated by GW-BSE and the Huang-Rhys (HR) formula is employed to calculate the peak shape connected with the FC effect. Due to the computational workload involved in the HR calculation, we adopt the present case as a good approximation to tread broadening and shape also for all the BT2N absorption spectra considered.

THEORETICAL METHOD

The ground state electronic and geometric properties of a single isolated BT2Na, BT2N and stacked BT2N systems have been obtained by density functional theory[19, 20] (DFT) with a generalized gradient approximation based on the Perdew-Burke-Ernzerhof formula[21](PBE) for the electron exchange and correlation potential $V_{xc}[n(\mathbf{r})]$, and norm-conserving pseudopotentials have been constructed with the Troullier-Martins scheme[22] in the framework of a plane-wave basis set expansion. DFT calculations have been performed using the QUANTUM-ESPRESSO package[23], with a plane-wave energy cutoff of 70 Ry for the wave functions. Structural optimization has been achieved in a cubic box of 20x40x20 $\mathring{A}^3$ using the Broyden-Fletcher-Goldfarb-Shanno (BFGS) method[24] together with the Hellmann-Feynman forces acting on the ions; an empirical dispersion forces [25] is included to handle the long range interactions (π stacking) between the molecules. The chosen box size is large enough to prevent any spurious interaction arising from the effects of the periodically repeated images of the molecules. Concerning BT2Na, the atomistic configuration of the excited state has been obtained in the same context and with the same parameters as the ground state, but with a constrained occupation with both the HOMO and the LUMO occupied by one electron. While this approach is, in general, wrong, it has been demonstrated that it leads to an atomistic configuration quite close to the real one of the excited state if it is characterized by a single, well defined transition[16], as in the present case (see below). All the calculations have been performed using the Γ point for the Brillouin zone sampling, and the ionic minimization was done until the convergence threshold of 0.001 a.u. for the total force was achieved. Theoretical band gaps have been obtained with three different levels of accuracy: in the context of ground state DFT either as the difference between the lowest unoccupied molecular orbital (LUMO) and the highest occupied molecular orbital (HOMO) (simply referred as ε_{gap}), or as the difference between the electron affinity and the ionization potential $\varepsilon_{gap}^{\Delta SCF} = E_{N+1} - E_N - (E_N - E_{N-1})$ (the so called Δ-SCF method) where E_x is the DFT ground state total energy of the system containing x electrons [26], and lastly through the GW method that allows the calculation of the quasi-particle (QP) energies in the context of MBPT; the last task has been attained using the YAMBO code[27]. In particular, QP energies are computed to first order as:

$$\varepsilon_n^{\mathrm{QP}} = \varepsilon_n^{(0)} + Z_n \langle n|[\Sigma(\varepsilon_n^{(0)}) - V_{xc}]|n\rangle \tag{1}$$

where $\varepsilon_n^{(0)}$ and $\langle \mathbf{x}|n\rangle = \phi_n(\mathbf{r})$ are the eigenvalues and eigenfunctions of the DFT hamiltonian respectively, and

$$Z_n = \left(1 - \frac{\partial \Sigma_n}{\partial \omega}\bigg|_{\omega=\varepsilon_n^{(0)}}\right)^{-1} \tag{2}$$

where $\Sigma_n(\omega) = \langle n|\Sigma(\mathbf{r}_1\mathbf{r}_2, \omega)|n\rangle$ is the Fourier transform of the dynamical electron self-energy operator Within the GW approximation[28], $\Sigma(\mathbf{r}_1\mathbf{r}_2, \omega)$ can be cast in terms of the ground state DFT Green's function $G(\mathbf{r}_1\mathbf{r}_2, \omega)$ as:

$$\Sigma(\mathbf{r}_1\mathbf{r}_2, \omega) = i\lim_{\eta\to 0^+} \int \frac{d\omega'}{2\pi} e^{i\omega'\eta} G(\mathbf{r}_1\mathbf{r}_2, \omega - \omega') W(\mathbf{r}_1\mathbf{r}_2, \omega') \tag{3}$$

with

$$G(\mathbf{r}_1\mathbf{r}_2, \omega) = \lim_{\eta\to 0^+} \sum_n \frac{\phi_n(\mathbf{r}_1)\phi_n^*(\mathbf{r}_2)}{\omega - [\varepsilon_n^{(0)} + i\eta \mathrm{sgn}(\mu - \varepsilon_n^{(0)})]} \tag{4}$$

and

$$W(\mathbf{r}_1\mathbf{r}_2, \omega) = \int d\mathbf{r}_3 \frac{\epsilon^{-1}(\mathbf{r}_3\mathbf{r}_2, \omega)}{|\mathbf{r}_1 - \mathbf{r}_3|} \tag{5}$$

is a dynamically screened interaction, expressed in terms of the inverse dielectric function ϵ^{-1} of the system and of the bare Coulomb interaction V.

The inverse dielectric matrix is related to the response function $\chi(12) = \delta\rho(1)/\delta V_{ext}(2)$ (where (1) is a short-hand notation for $(\mathbf{r}_1, t_1)$) via the relation:

$$\epsilon^{-1}(12) = \delta(12) + \int d(3) \frac{\chi(32)}{|\mathbf{r}_1 - \mathbf{r}_3|} \tag{6}$$

In the RPA approximation[27], χ is related to the non-interacting response function $\chi^{(0)}(12) = G(12)G(21^+)$, through the Dyson-like equation:

$$\chi(12) = \chi^{(0)}(12) + \int d(34)\chi^{(0)}(13) \frac{1}{|\mathbf{r}_3 - \mathbf{r}_4|} \chi(42) \tag{7}$$

Another common approximation for the screened interaction is the plasmon pole approximation (PPA)[27, 29], in which it is assumed that the imaginary part of W is characterized by a strong peak corresponding to a plasmon excitation at the plasmon frequency; both methods (the GW-RealAxis and the GW-PPA schemes in the following), will be employed to evaluate the quasiparticle corrections to DFT energy gaps. The reader is referred to the recent literature for details on the calculation parameters [18]

Using the above obtained dynamically screened interaction, the macroscopic complex dielectric function that includes the excitonic effects is obtained by solving BSE in the electron-hole (e-h) space made of e-h pairs $|eh\rangle$ and antipairs $\overline{|he\rangle}$; its solution, in fact, can be mapped onto an eigenvalue problem for a two particle excitonic Hamiltonian[30, 31] of the form:

$$\mathcal{H}^{\text{exc}} = \begin{bmatrix} H^{\text{res}} & H^{\text{coupl}} \\ -(H^{\text{coupl}})^* & -(H^{\text{res}})^* \end{bmatrix} \tag{8}$$

where the resonant term $H^{\text{res}} = (E_e - E_h)\delta_{e,e'}\delta_{h,h'} + \langle eh|K|e'h'\rangle$ is Hermitian, the coupling part $H^{\text{coupl}} = \langle eh|K|\overline{h'e'}\rangle$ is symmetric, and $K = W - 2V$ is the excitonic kernel (the reader is referred to [31] for a detailed explanation of the block terms in $\mathcal{H}^{\text{exc}}$).

The macroscopic dielectric function $\epsilon_M(\omega)$ is calculated from the eigenvalues E_λ and the eigenstates $|\lambda\rangle$ of $\mathcal{H}^{\text{exc}}$ as:

$$\epsilon_M(\omega) = 1 - \lim_{\mathbf{q}\to 0} \lim_{\eta\to 0^+} v_0(\mathbf{q}) \sum_{\lambda\lambda'} \left(\sum_{n_1 n_2} \langle n_1|e^{-i\mathbf{q}\cdot\mathbf{r}}|n_2\rangle \frac{A^{\lambda}_{n_1 n_2}}{\omega - E_\lambda + i\eta} \right.$$
$$\left. \times S^{-1}_{\lambda\lambda'} \sum_{n_3 n_4} (f_{n_4} - f_{n_3}) \langle n_4|e^{i\mathbf{q}\cdot\mathbf{r}'}|n_3\rangle (A^{\lambda'}_{n_3 n_4})^* \right) \tag{9}$$

with $A^{\lambda}_{nn'} = \langle nn'|\lambda\rangle$, and $S_{\lambda\lambda'}$ is an overlap matrix of the generally non-orthogonal eigenstates of $\mathcal{H}^{\text{exc}}$.

Lastly we calculate the absorption spectra from the imaginary part of the system polarizability along the molecule axis (the transverse polarizability $\alpha_\perp$ figures out to be with respect to $\alpha_\parallel$) obtained through the Clausius-Mossotti relations[17]:

$$\alpha_\parallel = \frac{3\Omega}{4\pi} \frac{\epsilon_\parallel - 1}{\epsilon_\parallel + 2} \tag{10}$$

Dynamical effects in the excitonic hamiltonian have been neglected, since it has been shown[16] that they affect optical gaps of oligothiopehens by a small uniform reduction of 0.1 eV in the corresponding optical gaps. The absorption peak broadening and shape depends on the vibrational properties and has been calculated in the context of Density Functional Perturbation Theory. Indeed the FC effect can be calculated through the HR of method as [32]: the spectral function (SF) of the electron-local vibrations coupling is:

$$S(\hbar\omega) = \sum_\lambda S_\lambda \delta(\hbar\omega - \hbar\omega_\lambda) \tag{11}$$

The sum is over all the vibration modes λ of energy $\hbar\omega_\lambda$ and S_λ is the partial SF of the λ mode is defined as:

$$S_\lambda = \frac{\omega_\lambda q_\lambda^2}{2\hbar} \tag{12}$$

where

$$q_\lambda^2 = \sum_{\alpha i} m_\alpha^{1/2}(R_{I,\alpha i} - R_{N,\alpha i})\Delta r_{\lambda,\alpha i} \tag{13}$$

$m_{\alpha i}$ is the mass of the atom α, $i =, x, y, z$, $R_{[N,I]\alpha i}$ are the equilibrium positions of the atoms in the neutral [N] and the ionized [I] configurations, $\Delta r_{\lambda,\alpha i}$ is a normalized vector (expressed in mass reduced coordinates) representing the atomic displacements of the atom α along the i direction of the λ mode. It can be shown [33] that the absorption peak is obtained from the quasi-particle excitation energy spectrum convoluted with the function $A(\hbar\omega)$:

$$A(\hbar\omega) = \frac{S^n}{\Gamma(n+1)}\delta(\hbar\omega - n\hbar\bar{\omega}) \quad n = 0, 1, \ldots \tag{14}$$

with $\bar{\omega} = \frac{1}{S}\sum_\lambda \omega_\lambda S_\lambda$.

Result and Discussion

The ground state configurations of BT2Na and BT2N, the last one either isolated or π stacked are shown in Fig 1. Some important structural data including bond lengths and angles are reported in Table **??** were some differences between BT2N and BT2Na are found in the thiophene groups. The corresponding band gap data reported in Table 2. Isolated BT2N and BT2Na show the same band gap value obtained at the DFT-PBE theory level. Indeed it has been shown that the HOMO and LUMO orbitals in isolated BT2N are spread along the molecule axis but do not affect the aliphatic chains that have been removed in the case of BT2Na [18].

TABLE 1: Some relevant structural data of isolated BT2N, BT2Na and the BT2Na excited configurations.Bond lengths are in nm

Molecule	C_1-C_2	C_1-S_1	C_2-S_1	C_3-C_4	C_3-C_4	$\hat{\alpha_1}$	$\hat{\alpha_2}$
BT2N	0.145	0.171	0.177	0.141	0114	92.5	111.1
BT2Na	0.144	0.174	0.175	0.14	0.1139	93.2	113.4
BT2Na-exc	0.141	0.176	0.176	0.142	0.1138	92.9	114.3

The BT2N/BT2Na chemical structures suggests a typical acceptor-donor-acceptor (A-D-A) configuration; such an A-D-A character emerges from the orbital localization, even though it is not marked probably because of the reduced length size of the molecule; indeed previous studies [18] have shown that the HOMO is only partially localized on the electron-donating unit (i.e. the two central thiophene units) and the HOMO state is almost equally spread between the electron accepting and donating parts of the molecule while the LUMO is preferentially located at the acceptor ends of the molecule. As expected, the HOMO-LUMO gap is largely underestimated (being nearly of 1.39 eV for both the isolated molecules) at the DFT-PBE level with respect to the experimental value obtained for BT2N by CV (see Table 2) [18].

TABLE 2: DFT-PBE band gap energies of BT2N (π-stacked BT2N molecules in parenthesis) and BT2Na molecules. Experimental values for BT2N molecules are taken from the literature [18]

Molecule	DFT-PBE	Exp.	Chemical formula
BT2N	1.39 (1.30)	2.02	$C_{44}H_{52}N_2O_4S_4$
BT2Na	1.389	-	$C_{28}H_{20}N_2O_4S_4$

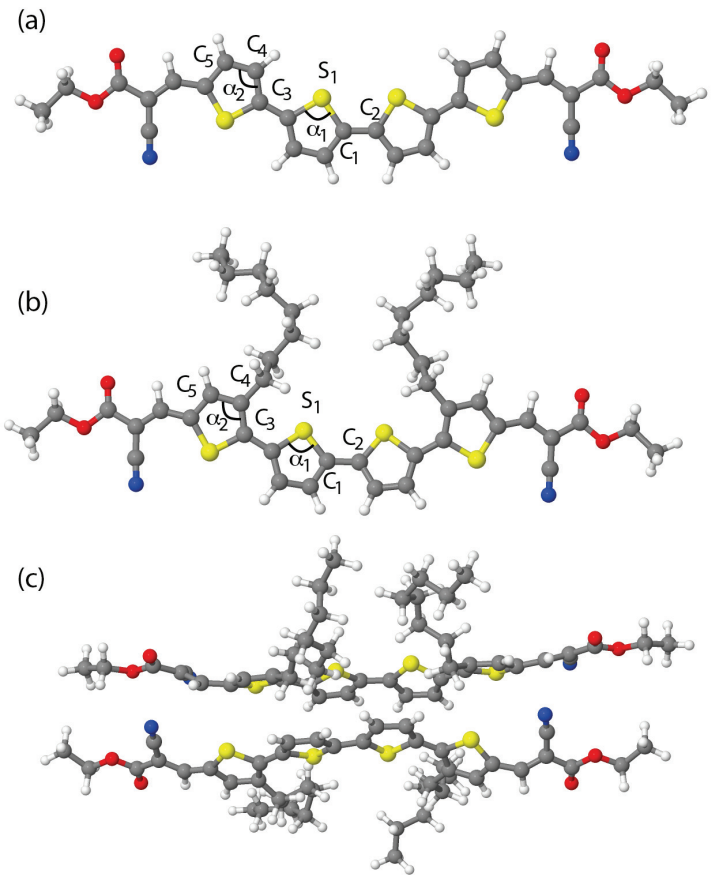

FIGURE 1: (Color online) Different ground state configurations isolated BT2Na (a) and BT2N (b) and π-stacked BT2N molecules.

The correct theoretical band gap are obtained from quasi-particle band gaps, calculated by GW (with either GW-RealAxis or GW-PPA approximation) and are reported in Table 3. We see that BT2Na has a slightly larger theoretical QP band-gap that the BT2N molecule. Previous studies have demonstrated that GW quasi-particle band gaps, that are theoretically correct, severely overestimate the experimental absorption peak of BT2N, that is a clear sign of excitonic behaviour of the absorbance phenomenon.

TABLE 3: Band Gaps (in eV) for the BT2N structures studied obtained with three different computational schemes.

Structure	GW-RealAxis	GW-PPA	Δ-SCF
BT2N	3.84	3.93	3.89
BT2Na	-	4.04	-
BT2Nx2	3.52	3.60	3.33

Therefore the absorption peak has been calculated by solving the BSE starting from both GW-PPA and GW-RealAxis energy levels; concerning isolated BT2N, we know that the absorption peak calculated from BSE starting from the GW-PPA is red-shifted from the experimental absorption peak by nearly $\Delta\lambda \sim 50$ nm while the situation is worse in the case of the BSE absorption peak obtained from the GW-RealAxis QP energy levels that are red-shifted by $\Delta\lambda \sim 100$ nm. Indeed, the calculated values of the QP electronic gap (3.93 eV and 3.84 eV for GW-PPA and GW-RealAxis respectively) are much larger than the optical band gap obtained from the optical spectrum, it is clear that the calculated optical spectrum reflects the existence of strong excitonic transitions, with high excitonic binding energy (1.92 eV and 1.96 eV for GW-PPA+BSE and GW-RealAxis+BSE, respectively) that is found to be entirely associated to single particle $\pi \rightarrow \pi^*$ transition from the HOMO to the LUMO levels.

The difference of the calculated absorption peak with respect to the experimental one has been attributed to the π stacking arrangement of the molecules [18]. Indeed the experimental peak energy is fully recovered by considering the absorption in π stacked molecules where the GW corrections to DFT-PBE energies, with both GW-RealAxis and GW-PPA schemes, result in a gap opening ($\varepsilon^{\mathrm{QP}}_{gap}$ =3.6 eV for GW-RealAxis and 3.5 eV for GW-PPA). The experimental absorption main peak is, indeed, obtained by solving the BSE using the GW-RealAxis approximation of the GW QP levels thus showing the fundamental importance of the local molecular ordering. This order, indeed, affects the main HOMO-LUMO transition because it has been demonstrated that the two molecular orbitals involved reside onto adjacent molecules thus involving a charge transfer. Moreover also other transitions contribute to the absorption peak lying on the two adjacent BT2N molecules.

The above discussed data concerns only the absorption peaks and do not account for the peak shape and broadening that is due to the FC effect depending on the vibrational modes of the molecules. The peak broadening has been calculated using the approximate HR formula Eq. 14 and the local vibrational spectra have been calculated with reference to the modified BT2Na molecule, i.e. the simplified version of the BT2N molecule obtained by removing the aliphatic chain. This choice is basically justified by the fundamental argument that the MO involved in the absorption are, in all the cases treated, even in the case of the π stacked geometry, located along the tiophene chain and do not affect significantly the aliphatic chains. Of course the vibrational spectra of the molecules might be affected by the aliphatic chains vibrations also but, due to the strong bonding of the central thiophenes, we are confident that the local vibrational spectra should be only slightly affected by the aliphatic chains. As mentioned in the section a), the molecular configuration of the excited state has been obtained by an occupation constrained optimization of the BT2Na molecule. Indeed it has been demonstrated that, while this method is rigorously wrong from a theoretical point of view, the atomistic configuration of the pseudo-excited state obtained with a constrained occupation with both the HOMO and the LUMO occupied by one electron is rather close to the one of the real excited state if this excited state is characterized by a single, well defined transition, that is exactly the present case for isolated BT2N and BT2Na molecules [16]. Of course this is not the case for the π-stacked BT2N configuration that just means that the atomic configuration of the excited state, needed to calculate the HR SF, in this case cannot be obtained with the same method. The structural data of the excited BT2Na molecule are reported in Table **??** and show that the central C_1-C_2 bond is shortened, while the two central thiophenes are elongated with respect to the ground state configurations. The local vibrational spectrum, needed in the HR formula, is calculated in the context of the DFPT and the partial HR factors are calculated from Eq. 12. Both of them are reported in Fig. 2 and show that there are two main modes involved in the peak broadening located at 780 THz and 1410 THz with partial HR factors of $S_\lambda \approx 0.23$ and $S_\lambda \approx 0.22$ respectively. Moreover there are also other, less important, modes at 120, 550 and 580 THz with partial HR factors of $S_\lambda \approx 0.13$ and $S_\lambda \approx 0.1$.

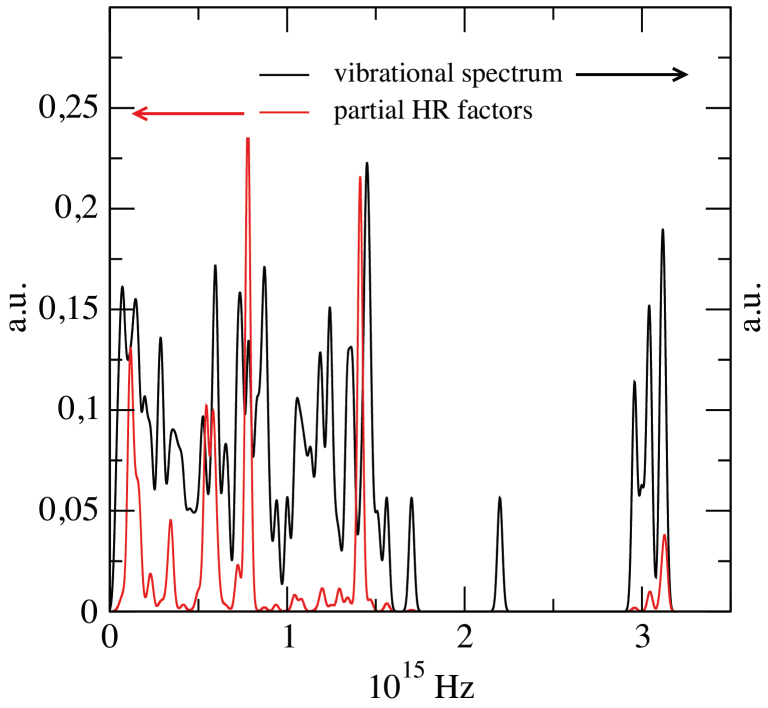

FIGURE 2: (Color Online) Local vibrational spectrum of the BT2Na molecule calculated by DFPT and the partial HR factors.

The whole HR factors is $S \approx 1.15$ indicating that, in average, one vibrational mode affect the peak broadening. The HR broadened absorptions spectra of isolated BT2N and BT2Na molecules are reported in Fig. 3. The absorption spectra, that have been normalized to their maxima, show that, at the GW-PPA+BSE level of theory, the two molecules BT2N and BT2Na have the same absorption peak calculated starting from the PPA of the GW QP energy. The BT2N and the BT2Na have rather close values of the HR broadening also. In the seme figure is reported the absorption peak of the isolated BT2N molecule calculated using the RealAxis approximation of the GW QP energy. The full width at half maximum (FWHM) measured for BT2N in both the employed approximations is $\Delta E_{FWHM} \approx 0.40eV$ while for BT2Na is nearly $100meV$ smaller mainly because in this case we have not employed an artificial broadening that simulates the collision and rotation effects. The HR factor causes a small shift of the absorption peak maximum to larger energy so that $\alpha_{max} \approx 2.13eV$ instead of the nominal $\alpha_{max} \approx 2.05eV$ of the peak position obtained from the GW-PPA+BSE level of the theory. Nevertheless we see from Fig. 4 that this shift is not sufficient to fully recover the experimental absorption peak position already reported in the literature. The same HR factor is, then, applied to the absorption peak obtained in the case of two π-stacked BT2N molecules that, as reported in the recent literature, show the existence of two, very close peaks exactly at the experimental absorption peak and an additional one at $E \approx 2eV$. The absorption peak obtained from the calculated HR factor, again shown in Fig. 4 has the correct position but its width is severely underestimated with a FWHM of $\Delta E \approx 260meV$ instead of the experimental $\Delta E \approx 650meV$. We see, however that a superposition of the two peaks accounts for the main peak position and its largest satellite and that the sum of the two peak widths is consistent with the experimental measured absorpion peak width. Therefore it is likely that the experimental absorption spectrum features, namely the main peak position, additional satellites, the peak broadening and shape, could be explained through an appropriate superposition of the absorption characteristics of both the isolated and the π-stacked BT2N molecules.

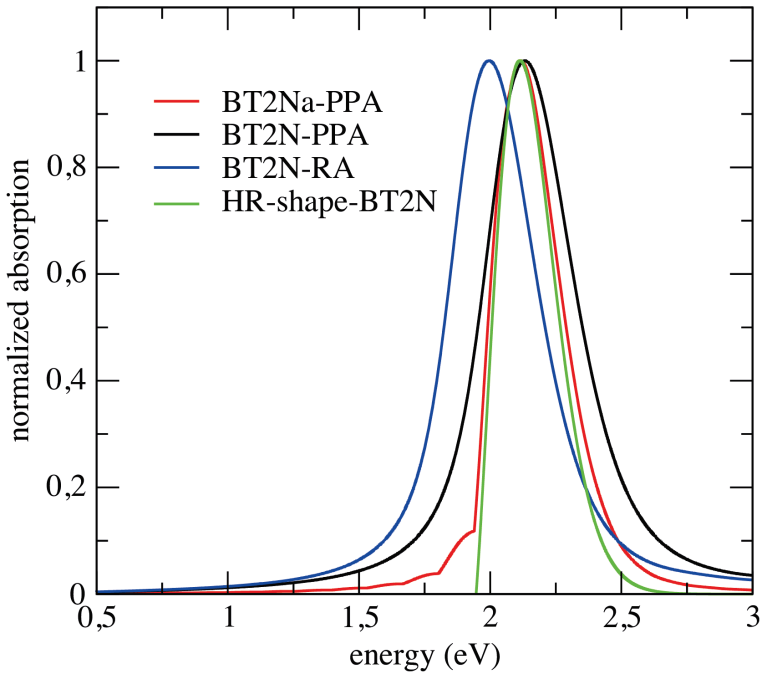

FIGURE 3: (Color online) Normalized absorption of light polarized parallel to the main axis of the molecule for spectra for BT2N and BT2Na isolated molecules. In the same figure the HR broadening and peak shape is reported calculated for an ideal absorption with one peak with zero standard deviation at $E = 2.05eV$.

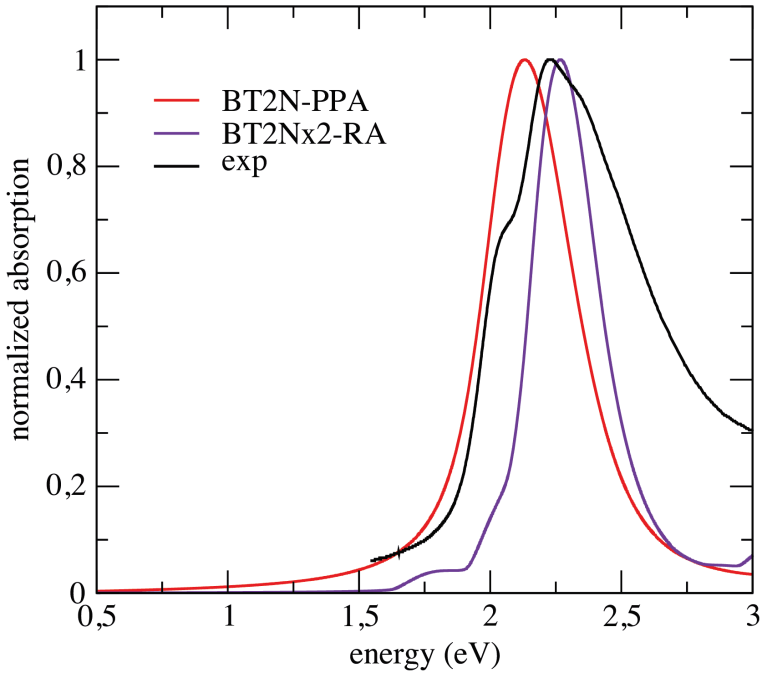

FIGURE 4: (Color online) Normalized absorption of light polarized parallel to the main axis of the molecule for spectra for BT2N and two π-conjugated molecules compared to the experimental absorption peak [18].

Conclusions

In summary we have calculated in the context of the MBPT, using the GW approximation and the BSE for the excitonic Hamiltonian, the absorption spectra of two different systems made either of one isolated BT2N or BT2Na molecule or two π conjugated BT2N molecules evidencing the the excitonic nature of the measured absorption onset and main peak. Moreover we have calculated the FC broadening of the absorption peak on the basis of the HR formula. The absorption peaks of the isolated BT2N and BT2Na molecules are quite similar thus enforcing the idea that, in spite of the slight differences found for the ground sate configurations of theses two molecules, the absorption phenomena is entirely confined in the main molecular axis with thiophene groups. The theoretical absorption spectrum of BT2N and BT2Na have been discussed and, by including an artificial broadening that accounts for the molecular rotation and collisions, the simplified HR factor accounts for a peak broadening of nearly $\Delta E_{FWHM} \approx 400meV$ that is still unfit to explain the broadening and the shape of the experimental results. However the HR factor broadening causes a shift of the single molecule absorption peak to higher energy by nearly $\Delta E_{shift} \approx 80meV$. In previous articles it has been shown that π conjugated geometry of BT2N molecules should be considered in order to recover the absorption energy of the main peak showing that inter-molecular transitions are needed to recover the peak position. However, playing with shape and broadening caused by the FC effect, a strong indication is obtained that the peak shape and broadening could be explained invoking both inter-molecular and intra-molecular transitions of both isolated and π-conjugated molecules. Further studies are in course to better clarify this aspect.

ACKNOWLEDGMENTS

Computational resources have been provided by CRESCO/ENEAGRID High Performance Computing infrastructure and its staff [34]. CRESCO/ENEAGRID High Performance Computing infrastructure is funded by ENEA, the Italian National Agency for New Technologies, Energy and Sustainable Economic Development and by Italian and European research programmes, see http://www.cresco.enea.it/english for information. Part of the calculations have been performed using the NARTEN computational facility of the CNIS-Nanolab at the University ”La Sapienza”

REFERENCES

[1] L. Dou, J. You, Z. Hong, Z. Xu, G. Li, R. Street, and Y. Yang, Adv. Mater. **25**, 6642 (2013).
[2] A. Heeger, Adv. Mater **26**, 10 (2014).
[3] C.W.Tang, Appl. Phys. Lett. **48(2)**, 183 (1986).
[4] J.-L-Brédas, J. Norton, J. Cornil, and V. Coropceanu, Acc. Chem. Res. **42(11)**, 1691 (2009).
[5] Y. Liu, C.-C. Chen, Z. Hong, J. Gao, Y. Yang, H. Zhou, L. D. G. Li, and Y. Yang, Sci. Rep. **3356**, 3 (2013).
[6] B. Kan, Q. Zhang, M. Li, X. Wan, W. Ni, G. Long, Y. Wang, X. Yang, H. Feng, and Y. Chen, J. Am. Chem. Soc. **136**, 15529 (2014).
[7] Q. Zhang, B. Kan, F. Liu, G. Long, X. Wan, X. Chen, Y. Zuo, W. Ni, H. Zhang, M. Li, et al., Nature Photonics **9**, 35 (2015).
[8] B. Kan, M. Li, Q. Zhang, F. Liu, X. Wan, Y. Wang, W. Ni, G. Long, X. Yang, H. Feng, et al., J. Am. Chem. Soc. **137**, 3886 (2015).
[9] H. Bai, Y. Wang, P. Cheng, Y. Li, D. Zhu, and X. Zhan, ACS Appl. Mater. Interfaces **6(11)**, 8426 (2014).
[10] Y. ad G.C. Welch, W. L. Leong, C. Takacs, and G. Bazan, Nature Materials **11**, 44 (2012).
[11] D. Patra, T.-Y. Huang, C.-C. Chiang, R. Maturana, C.-W. Pao, K.-C. Ho, K.-H. Wei, and C.-W. Chu, ACS Appl. Mater. Interfaces **5**, 9494 (2013).
[12] L. Hedin, Phys. Rev. **139**, A796 (1965).
[13] C. P., M. Gatti, and A. Rubio, Phys. Rev. B **86**, 195307 (2012).
[14] S. Sharifzadeh, A. Biller, L. Kronik, and J. B. Neaton, Phys. Rev. B **85**, 125307 (2012).
[15] M. Palummo, C. Hogan, F. Sottile, P. Bagalá, and A. Rubio, J. Chem. Phys. **131**, 084102 (2009).
[16] B. Baumeier, D. Andrienko, Y. Ma, and M. Rohlfing, J. Chem. Theory Comput. **8**, 997 (2012).
[17] C. Hogan, M. Palummo, J. Gierschner, and A. Rubio, J. Chem. Phys. **138**, 024312 (2013).
[18] F. Gala, L. Mattiello, F. Brunetti, and G. Zollo, J. Chem. Phys. **144**, 084310 (2016).
[19] P. Hohenberg and W. Kohn, Phys. Rev. **136**, B864 (1964), URL `http://link.aps.org/doi/10.1103/PhysRev.136.B864`.
[20] W. Kohn and L. J. Sham, Phys. Rev. **140**, A1133 (1965), URL `http://link.aps.org/doi/10.1103/PhysRev.140.A1133`.
[21] J. Perdew, K. Burke, and M.Ernzerhof, Phys. Rev. Lett. **77(4)**, 3865 (1996).
[22] N. Troullier and J. Martins, Phys. Rev. B **43(14)**, 1993 (1991).
[23] P. Giannozzi, S. Baroni, N. Bonini, M. Calandra, R. Car, C. Cavazzoni, D. Ceresoli, G. L. Chiarotti, M. Cococcioni, I. Dabo, et al., J. Phys.: Condens. Matter **21(19)**, 395502 (2009).
[24] R. Fletcher, The Computer Journal **13(6)**, 317 (1970).
[25] S. Grimme, J. Comput. Chem. **27(15)**, 1787 (2006).
[26] R. M. Martin, *Electronic Structure: Basic Theory and Practical Methods* (Cambridge University Press, 2008).
[27] A. Marini, C. Hogan, M. Grüning, and D. Varsano, Comput. Phys. Comm. **180**, 1392 (2009).
[28] L. Hedin and S. Lundqvist, *Solid State Physics: Advances in Research and Application* (Academic Press: New York, San Francisco, London, 1969).
[29] F. Aryasetiawan and O. Gunnarsson, Rep. Prog. Phys. **61**, 237 (1998).
[30] M. Rohlfing and S. G. Louie, Phys. Rev. B **62(8)**, 4927 (2000).
[31] G. Onida, L. Reining, and A. Rubio, Rev. Mod. Phys. **74**, 601 (2002).
[32] K. Huang and A. Rhys, Proc. Roy. Soc. **204**, 407 (1970).
[33] A. Gali, T. Demián, M. Vörös, G. Thiering, E. Cannuccia, and A. Marini, Nat. Comm. **7**, 11327 (2016).
[34] G. Ponti, F. Palombi, D. Abate, F. Ambrosino, G. Aprea, T. Bastianelli, F. Beone, R. Bertini, G. Bracco, M. Caporicci, et al., IEEE HPCS **6903807**, 1030 (2014).